Genetic Defect in Phospholipase Cδ1 Protects Mice From Obesity by Regulating Thermogenesis and Adipogenesis

Masayuki Hirata,[1] Mutsumi Suzuki,[1] Rika Ishii,[1] Reiko Satow,[1] Takafumi Uchida,[1] Tomoya Kitazumi,[2] Tsutomu Sasaki,[2] Tadahiro Kitamura,[2] Hideki Yamaguchi,[3,4] Yoshikazu Nakamura,[1] and Kiyoko Fukami[1]

OBJECTIVE—Regulation of obesity development is an important issue to prevent metabolic syndromes. Gene-disrupted mice of phospholipase Cδ1 (*PLCδ1*), a key enzyme of phosphoinositide turnover, seemed to show leanness. Here we examined whether and how PLCδ1 is involved in obesity.

RESEARCH DESIGN AND METHODS—Weight gain, insulin sensitivity, and metabolic rate in *PLCδ1*$^{-/-}$ mice were compared with *PLCδ1*$^{+/-}$ littermate mice on a high-fat diet. Thermogenic and adipogenetic potentials of *PLCδ1*$^{-/-}$ immortalized brown adipocytes and adipogenesis of *PLCδ1*-knockdown (KD) 3T3L1 cells, or *PLCδ1*$^{-/-}$ white adipose tissue (WAT) stromal-vascular fraction (SVF) cells, were also investigated.

RESULTS—*PLCδ1*$^{-/-}$ mice showed marked decreases in weight gain and mass of epididymal WAT and preserved insulin sensitivity compared with *PLCδ1*$^{+/-}$ mice on a high-fat diet. In addition, *PLCδ1*$^{-/-}$ mice have a higher metabolic rate such as higher oxygen consumption and heat production. When control immortalized brown adipocytes were treated with thermogenic inducers, expression of PLCδ1 was decreased and thermogenic gene uncoupling protein 1 (*UCP1*) was upregulated to a greater extent in *PLCδ1*$^{-/-}$ immortalized brown adipocytes. In contrast, ectopic expression of PLCδ1 in PLCδ1$^{-/-}$ brown adipocytes induced a decrease in UCP expression, indicating that PLCδ1 negatively regulates thermogenesis. Importantly, accumulation of lipid droplets was severely decreased when *PLCδ1*-KD 3T3L1 cells, or *PLCδ1*$^{-/-}$ WAT SVF cells, were differentiated, whereas differentiation of *PLCδ1*$^{-/-}$ brown preadipocytes was promoted.

CONCLUSIONS—PLCδ1 has essential roles in thermogenesis and adipogenesis and thereby contributes to the development of obesity. ***Diabetes*** **60:1926–1937, 2011**

Obesity is a growing concern in present society because it leads to many metabolic syndromes that are defined by visceral obesity complicated by type 2 diabetes, hypertension, and increased cardiovascular risk. White adipose tissue (WAT) functions as a lipid storage, insulin sensor, and endocrine organ that produce adipokines (1–4). An increase in the number and size of adipocytes is a hallmark of obesity. The former seems to be caused by proliferation and differentiation of preadipocytes. On the other hand, the diet-induced increase in cell size is characterized by adipocyte hypertrophy, which may be primarily caused by excessive lipid overload and a decrease in metabolic rate.

Brown adipose tissue (BAT) is implicated in thermogenesis and metabolic enhancement (5). Recent reports indicated that BAT and skeletal muscle originate from a common precursor cell (6–9). Like skeletal muscle, BAT plays a role in thermogenesis by promoting the expression of a thermogenic gene, uncoupling protein 1 (*UCP1*). Upregulation of *UCP1* by genetic manipulations or pharmacological agents has been shown to reduce obesity and improve insulin sensitivity (5). Other recent studies demonstrating that a considerable amount of metabolically active BAT exists in many adult humans have invoked an important and novel role of BAT as an anti-obesity agent (10,11). Therefore, understanding the development or functions of WAT and BAT is indispensable for preventing obesity.

Phosphoinositide metabolism plays crucial roles in diverse cellular functions, including cell growth, cell migration, endocytosis, and cell differentiation (12,13). Phospholipase C (PLC), a key enzyme in this system, catalyzes the hydrolysis of phosphatidylinositol 4,5-bisphosphate, leading to the generation of two second messengers, namely, diacylglycerol and inositol 1,4,5-triphosphate. Diacylglycerol stimulates protein kinase C (PKC) activation and inositol 1,4,5-triphosphate releases Ca^{2+} from the intracellular stores. Thirteen mammalian PLC isozymes have been identified and grouped into six classes, β, γ, δ, ε, ζ, and η, on the basis of their structure and regulatory mechanisms (14,15). Among these classes, the δ-type PLC is evolutionarily conserved and therefore expected to have important and basic physiological functions. We have generated δ-type PLC knockout ($^{-/-}$) mice and previously reported that PLCδ1 has an essential role in skin homeostasis (16–18).

Here, we report that *PLCδ1*$^{-/-}$ mice were protected from diet-induced obesity and show a higher metabolic rate. Expression of thermogenic gene *UCP1* was more enhanced in *PLCδ1*$^{-/-}$-immortalized brown adipocytes when cells were treated with thermogenic inducers, suggesting PLCδ1 has a role in thermogenesis. Furthermore, knockdown (KD) of *PLCδ1* in 3T3L1 preadipocytes, or *PLCδ1*$^{-/-}$ WAT stromal-vascular fraction (SVF), reduced the accumulation of lipid droplets during adipocyte differentiation in vitro, indicating that PLCδ1 is involved in adipogenesis.

RESEARCH DESIGN AND METHODS

Mice. *PLCδ1*$^{-/-}$ mice were generated previously and genotyped with tail by PCR using a mixture of the following three primers: forward (5′-CAAGGAGGTGAAGGACTTCCTG-3′), reverse (5′- CTGGGTCAGCATCCTGTAGAAG-3′),

From the [1]Laboratory of Genome and Biosignal, Tokyo University of Pharmacy and Life Sciences, Hachioji, Tokyo, Japan; the [2]Metabolic Signal Research Center, Institute for Molecular and Cellular Regulation, Maebashi, Gunma, Japan; the [3]Growth Factor Division, National Cancer Center Research Institute, Chuo-ku, Tokyo, Japan; and [4]PRESTO, Japan Science and Technology Agency, Kawaguchi-shi, Saitama, Japan.
Corresponding author: Kiyoko Fukami, kfukami@ls.toyaku.ac.jp.
Received 26 October 2010 and accepted 24 April 2011.
DOI: 10.2337/db10-1500
This article contains Supplementary Data online at http://diabetes.diabetesjournals.org/lookup/suppl/doi:10.2337/db10-1500/-/DC1.
M.H., M.S., and R.I. contributed equally to this work.

and neomycin (5′- CCTGTGCTCTAGTAGCTTTACG-3′) (16). Mice had ad libitum access to water and either regular diet (RD) (CLEA Rodent diet CE-2; 12.6% of calories from fat; CLEA Japan, Tokyo, Japan) or high-fat diet (HFD) (CLEA Rodent diet Quick Fat; 30.6% of calories from fat; CLEA Japan). For diet-induced obesity, the mice were fed with HFD from the age of 6 weeks to 27 weeks. We performed experiments with male mice.

Measurement of blood glucose, plasma insulin level, and plasma leptin. Blood glucose was measured directly with a blood glucose meter (Sanwa Kagaku Kenkyusho, Nagoya, Japan). Plasma insulin or leptin concentration was measured by an insulin ELISA kit or leptin ELISA kit (Shibayagi, Shibukawa, Japan). For glucose tolerance tests, mice were fasted for 16 h and injected intraperitoneally with glucose (2 g/kg body wt). For insulin tolerance tests, mice with ad libitum access to diets were intraperitoneally injected with human regular insulin (0.25 or 0.75 units/kg for RD or HFD, respectively; Eli Lilly, Indianapolis, IN).

Energy metabolism. The 24-week-old $PLC\delta1^{+/-}$ and $PLC\delta1^{-/-}$ mice fed with RD or HFD were subjected to metabolic analysis. Indirect calorimetry was performed with a computer-controlled open circuit calorimetry system (Oxymax; Columbus Instruments) composed of respiratory chambers. For measurement of oxygen consumption (VO_2) and carbon dioxide production (VCO_2), mice were individually housed in respiratory chambers to acclimate them for 1 day before measurement. Data were recorded for 2–3 days. Respiratory quotient was calculated as the VCO_2 to VO_2 ratio. Heat generation can also be calculated with the following expression: heat = calorie value × VO_2 (calorie value = 3.815 + 1.232 × VCO_2/VO_2).

Western blot analysis. Western blot analysis was carried out as described previously (18). Anti-PLCδ1 antibody was developed previously (18). Anti-UCP1 (Santa Cruz Biotechnology, Santa Cruz, CA), Tim23 (BD Biosciences, Tokyo, Japan), heat shock protein 60 (Hsp60) (Stressgen), cytochrome c (Cell Signaling), PKCβI (Santa Cruz Biotechnology), PKCε (Cell Signaling,), caveolin-1 (BD Biosciences), nuclear factor of activated T (NFAT)c4 (Santa Cruz Biotechnology), lamin B1 (Santa Cruz Biotechnology), and β-actin (Sigma, St. Louis, MO) antibodies were purchased, respectively.

Quantitative real-time PCR. Total RNAs from tissues and cells were isolated using an RNeasy Lipid tissue mini-kit or an RNeasy mini-kit (Qiagen, Venlo, the Netherlands). Template cDNA was synthesized from total RNA using the SuperScript III First-Strand Synthesis System (Invitrogen, San Diego, CA). Quantitative real-time PCR (qRT-PCR) was performed using a Thunderbird SYBR qPCR Mix (Toyobo, Osaka, Japan) with specific primer sets (Supplementary Table 1) in a CFX96 thermocycler (Bio-Rad, München, Germany). The relative amount of mRNA was normalized to *36B4* mRNA.

Retroviral infection. pMX-Ires Puro (IP) (19) was used to overexpress several genes, such as *PLCδ1*, or *SV40 large T antigen* into target cells. pSUPER retro puro (OligoEngine) was used for the expression of siRNA in target cells. The sequences used were as follows: scrambled (5′-GTAAGATGAGCTTCAAGGA-3′), 399i (5′-GGACCAGCGCAATACCCTA-3′), and 468i (5′-GGATAACAAGATGAACTTC-3′). For retrovirus preparation, indicated constructs were transiently transfected into the packaging cell line, PLAT-E cells (19) using Lipofectamine 2000 (Invitrogen). Target cells were maintained in a medium containing 1.5–2 μg/mL puromycin to select bulk cell populations stably transformed with the viruses.

Cell culture and adipocyte differentiation. 3T3L1 preadipocytes were cultured in Dulbecco's modified Eagle's medium (DMEM) with 10% calf serum. For adipocyte differentiation, 2-day postconfluent cells were maintained in DMEM containing 10% FBS, 5 μg/mL insulin, 0.3 mmol/L 3-isobutyl-1-methylxanthine (IBMX; Sigma), and 0.25 μmol/L dexamethasone for 3 days and incubated in DMEM with 10% FBS and 5 μg/mL insulin for an additional 4 days (20). Differentiated adipocytes were fixed with 4% paraformaldehyde and stained with 0.5% Oil Red O. For quantitative analysis, the lipid droplets were eluted with isopropylalcohol, and the absorbance was measured at 510 nm.

Isolation of WAT SVF and in vitro differentiation. SVF was prepared as reported previously (21). SVF cells were plated at 8×10^5 per well of a 24-well plate and grown in DMEM supplemented with 10% FBS and 10 ng/mL βFGF (R&D Systems, Minneapolis, MN). After 2 days of incubation, the cells were incubated in differentiation medium with 10% FBS, 1 μg/mL insulin, 0.5 mmol/L IBMX, and 0.25 μg/mL dexamethasone for 3 days and then with 10% FBS for an additional 4 days. Fluorescence-activated cell sorting (FACS) analysis was performed using FACSCanto (Becton Dickinson, Franklin Lakes, NJ) to define stem cells from WAT SVF cells by staining with Ter119-FITC and CD45-APC.

Isolation of mouse immortalized brown preadipocytes. Immortalized brown preadipocytes were obtained from interscapular BAT of newborn $PLC1^{+/-}$ mice and $PLC1^{-/-}$ mice littermates by collagenase digestion, immortalized by infection with SV40 large T antigen retrovirus, and selected by 2 μg/mL puromycin for at least 3 weeks (22). Seven immortalized brown preadipocyte lines were established from independent littermates. For differentiation, 2-day-confluent brown preadipocytes were incubated for 3 days in culture medium supplemented with 20 nmol/L insulin, triiodothyronine (T3; Sigma, St. Louis, MO), 0.125 mmol/L IBMX, 0.5 μmol/L dexamethasone, and 0.5 μmol/L indomethacin. Subsequently, the cells were maintained in culture medium supplemented with 20 nmol/L insulin and 1 nmol/L T3 for 4 days. To stimulate thermogenesis, differentiated brown adipocytes at the same degree were treated with 0.5 mmol/L cAMP and 0.1 mmol/L forskolin for 4 h.

Statistical analysis. Data are expressed as the mean ± SEM. Statistical significance was assessed using the Student t test. A P value of < 0.05 was considered statistically significant.

RESULTS

***PLCδ1*$^{-/-}$ mice showed decreased weight gain and less accumulation of lipid droplets in metabolic tissues on HFD.** Because we noticed that $PLC\delta1^{-/-}$ mice seem to be leaner than $PLC\delta1^{+/-}$ mice, we measured the body weights of mice fed with RD or HFD from the age of 6 weeks to 20 weeks. $PLC\delta1^{-/-}$ mice had a decreased body weight compared with $PLC\delta1^{+/-}$ littermate mice on both RD and HFD (Fig. 1*A*), suggesting that the absence of the *PLCδ1* gene conferred protection from obesity. Decreased body fat mass was also observed in $PLC\delta1^{-/-}$ mice. The weights of epididymal WAT (eWAT) and BAT were extremely lower in $PLC\delta1^{-/-}$ mice on both diets. The weight of the liver was also lower in $PLC\delta1^{-/-}$ mice on HFD, whereas those of most other tissues were almost the same (Fig. 1*B*). Chronic exposure of mice to HFD causes enlarged body mass and accumulation of lipids in eWAT, BAT, and liver. HFD induced increased mass of eWAT in $PLC\delta1^{+/-}$ mice but not in $PLC\delta1^{-/-}$ mice (Fig. 1*C*). Moreover, BAT and liver in $PLC\delta1^{-/-}$ mice on HFD were darker than those in $PLC\delta1^{+/-}$ mice, indicating less accumulation of lipid in these tissues (Fig. 1*D* and *E*). Hematoxylin/eosin staining revealed that adipocyte sizes of eWAT and BAT were extremely smaller in $PLC\delta1^{-/-}$ mice than in $PLC\delta1^{+/-}$ mice on HFD (Fig. 1*F* and *G*). All these data suggest that the absence of the *PLCδ1* gene prevents obesity.

Improved glucose tolerance and increased systemic insulin sensitivity in *PLCδ1*$^{-/-}$ mice fed with HFD. Excessive lipid accumulation and hypertrophy in adipose tissues cause insulin resistance, which leads to a compensatory increase in insulin secretion and a decrease in glucose uptake (1–4). Chronic exposure to HFD remarkably increased blood glucose and plasma insulin levels in the fasting state in $PLC\delta1^{+/-}$ mice (Fig. 2*A* and *B*). However, these increases were not observed in $PLC\delta1^{-/-}$ mice, demonstrating that $PLC\delta1^{-/-}$ mice might be protected from HFD-induced insulin resistance. Intraperitoneal injection of glucose induced comparable levels of increase in blood glucose in both $PLC\delta1^{+/-}$ and $PLC\delta1^{-/-}$ mice on RD; however, $PLC\delta1^{-/-}$ mice were more glucose tolerant than $PLC\delta1^{+/-}$ mice on HFD (Fig. 2*C*). Similarly, $PLC\delta1^{-/-}$ mice fed with HFD were more sensitive to intraperitoneal injection of insulin compared with $PLC\delta1^{+/-}$ mice in the insulin tolerance test (Fig. 2*D*). Plasma leptin was significantly lower in $PLC\delta1^{-/-}$ mice (Fig. 2*E*).

Enhanced metabolic rate in *PLCδ1*$^{-/-}$ mice. Obesity is primarily caused by an excess food intake relative to energy expenditure. $PLC\delta1^{-/-}$ mice had similar food intake compared with $PLC\delta1^{+/-}$ mice on either RD or HFD (Fig. 3*A*). We then examined whether $PLC\delta1^{-/-}$ mice would have a higher energy expenditure. $PLC\delta1^{-/-}$ mice showed a significant increase in oxygen consumption and heat production compared with $PLC\delta1^{+/-}$ mice (Fig. 3*B*). This result indicates that $PLC\delta1^{-/-}$ mice have a higher energy expenditure and therefore a higher metabolic rate. Because these enhancements were observed throughout the light and dark

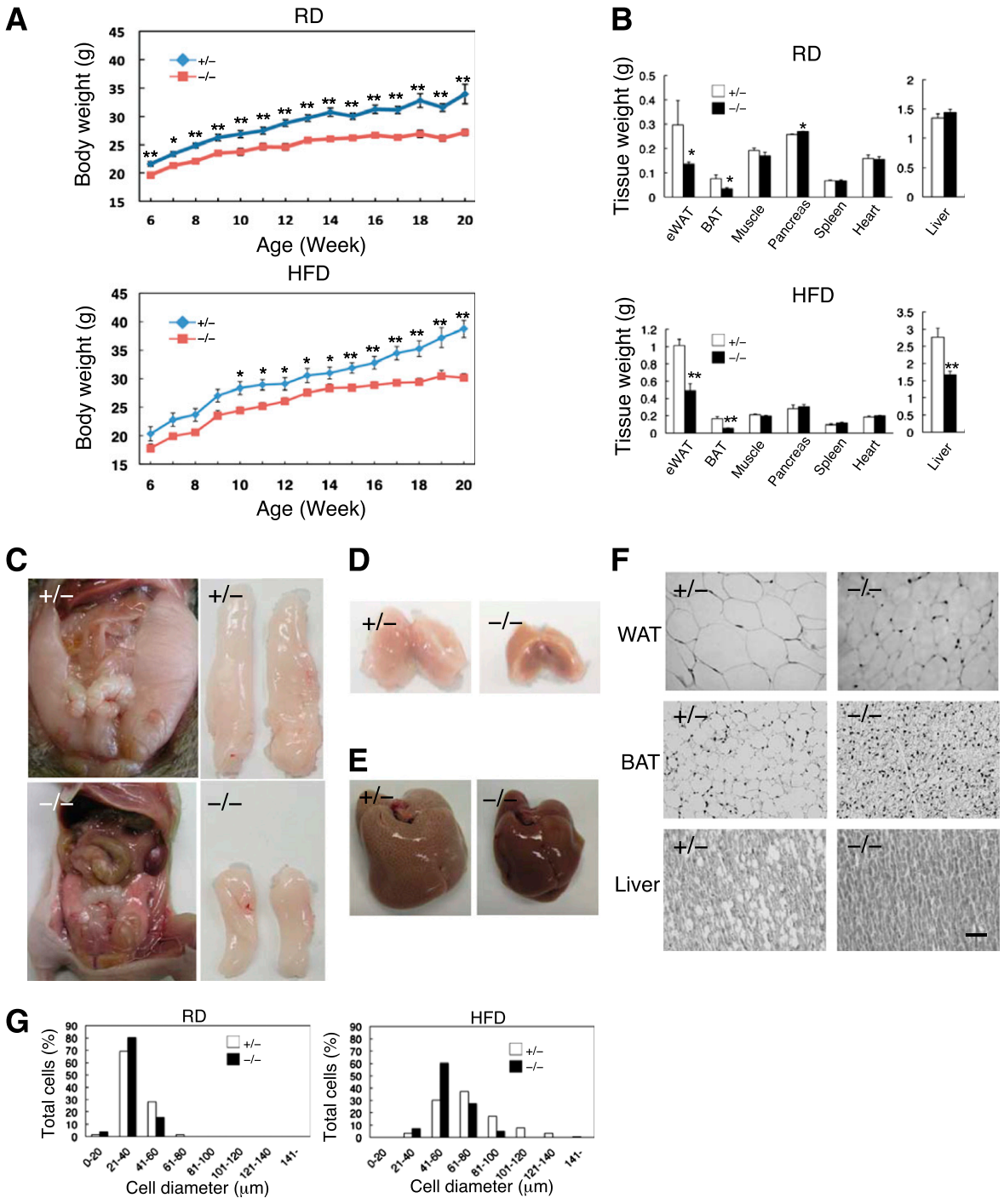

FIG. 1. ***PLCδ1*$^{-/-}$ mice are resistant to diet-induced obesity.** ***A*: Change in body weight of *PLCδ1*$^{+/-}$ (+/−) mice fed ad libitum with RD (n = 16) or HFD (n = 15) or *PLCδ1*$^{-/-}$ (−/−) mice fed RD (n = 13) or HFD (n = 15). *B*: Weight of various tissues from 24-week-old *PLCδ1*$^{+/-}$ mice fed RD (n = 3) or HFD (n = 9) or *PLCδ1*$^{-/-}$ mice fed RD (n = 7) or HFD for 18 weeks (n = 8). Tissue dissection of eWAT (*C*), BAT (*D*), and liver (*E*) from 24-week-old *PLCδ1*$^{+/-}$ or *PLCδ1*$^{-/-}$ mice fed HFD. *F*: Representative hematoxylin/eosin–stained sections of eWAT, BAT, and liver from 24-week-old *PLCδ1*$^{+/-}$ or *PLCδ1*$^{-/-}$ mice fed HFD. Scale bar, 50 μm. *G*: Distribution of adipocyte cell size in eWAT of *PLCδ1*$^{+/-}$ or *PLCδ1*$^{-/-}$ mice fed RD or HFD (n = 3). Cell diameter was measured. Values are expressed as the mean ± SEM. *P < 0.05, **P < 0.005. (A high-quality digital representation of this figure is available in the online issue.)**

phases, an increase in locomotion may not be involved. The respiratory quotient was also examined as a measure of fuel-partitioning patterns. No significant differences were observed between *PLCδ1*$^{+/-}$ and *PLCδ1*$^{-/-}$ mice either on RD or HFD (Fig. 3*B*).

PLCδ1 is highly expressed in WAT and BAT among metabolic tissues. Because WAT, BAT, liver, and skeletal muscle are involved in energy metabolism, we examined the expression pattern of *PLCδ1* among these metabolic tissues. qRT-PCR analysis showed that the relative expression level of *PLCδ1* was very high in WAT and BAT, low in muscles, and very low in the liver (Supplementary Fig. 1). This tissue-specific expression suggests that PLCδ1 possibly contributes to the pathogenesis of obesity-related metabolic disorders in adipose tissues.

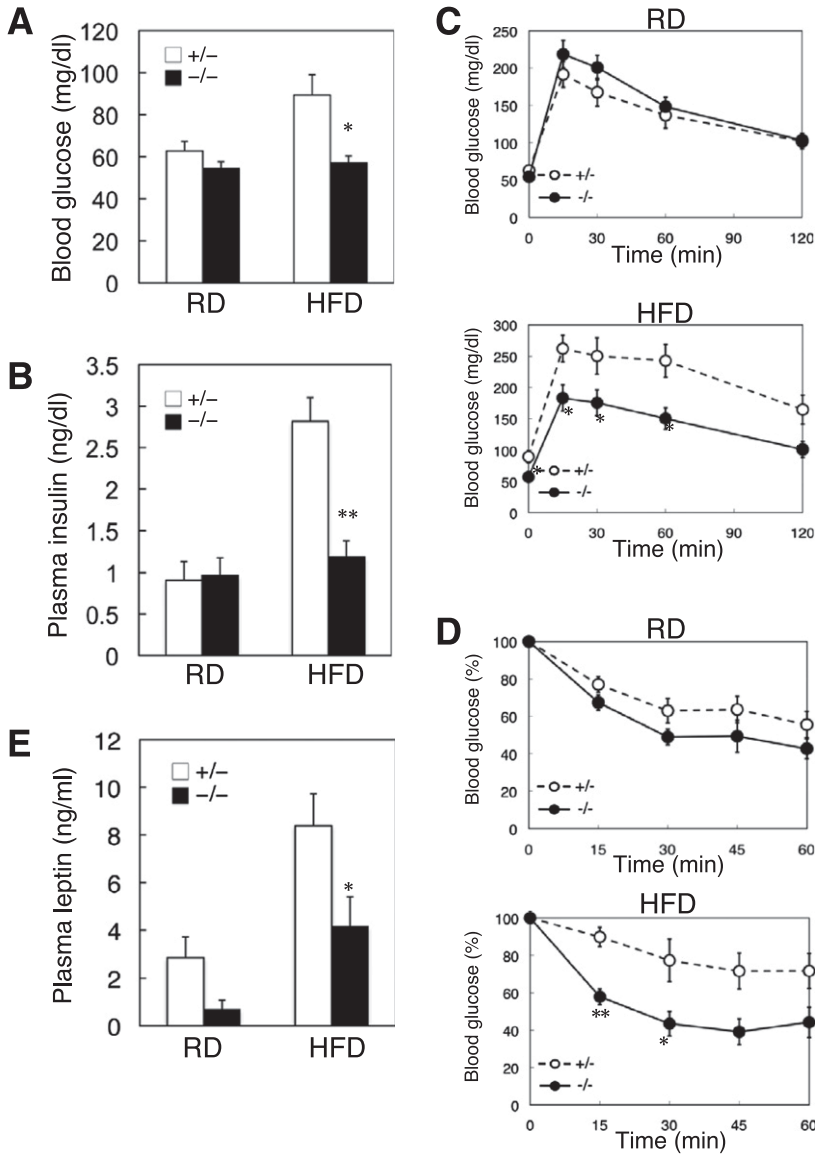

FIG. 2. Improved glucose tolerance and increased insulin sensitivity in $PLC\delta1^{-/-}$ mice fed HFD. *A*: Blood glucose levels in $PLC\delta1^{+/-}$ mice fed RD (n = 9) or HFD (n = 9) or $PLC\delta1^{-/-}$ mice fed RD (n = 11) or HFD for 18 weeks (n = 8) and then fasted for 16 h before measurement. *B*: Plasma insulin levels in $PLC\delta1^{+/-}$ mice fed RD (n = 8) or HFD (n = 6) or $PLC\delta1^{-/-}$ mice fed RD (n = 7) or HFD (n = 5) and then fasted for 16 h before measurement. *C*: Glucose tolerance test. Blood glucose levels after 16 h of fasting of $PLC\delta1^{+/-}$ mice fed RD (n = 9) or HFD (n = 9) or $PLC\delta1^{-/-}$ mice fed RD (n = 11) or HFD (n = 8) were measured at the indicated times after intraperitoneal injection with glucose. *D*: Insulin tolerance test. Blood glucose levels in $PLC\delta1^{+/-}$ mice fed RD (n = 9) or HFD (n = 9) or $PLC\delta1^{-/-}$ mice fed RD (n = 11) or HFD (n = 8) were measured at the indicated times after intraperitoneal injection with insulin. The level in time 0 is defined as 100%, and relative values are expressed. *E*: Plasma leptin levels in $PLC\delta1^{+/-}$ mice fed RD (n = 8) or HFD (n = 6) or $PLC\delta1^{-/-}$ mice fed RD (n = 7) or HFD (n = 5) and then fasted for 16 h before measurement. Values are expressed as the mean ± SEM. *$P < 0.05$, **$P < 0.005$.

Gene expression pattern of $PLC\delta1^{-/-}$ adipose tissues shows improved glucose and fat metabolism on HFD. Given that we observed inhibition of WAT hypertrophy, better glucose tolerance, and increased insulin sensitivity in $PLC\delta1^{-/-}$ mice, we examined the expression patterns of genes related to energy metabolism in WAT from mice aged 8 and 24 weeks on HFD by qRT-PCR analysis (Fig. 4*A* and Supplementary Fig. 2*A*). In 24-week-old $PLC\delta1^{-/-}$ mice, the expression of peroxisome proliferator–activated receptor γ (*PPARγ*) was increased, whereas *p21*, which is related to WAT hypertrophy (23), was extremely reduced compared with $PLC\delta1^{+/-}$ mice. The expression of genes related to glucose uptake, including glucose transporter 4 (*GLUT4*), Krüppel-like zinc finger transcription factor (*KLF15*), and *adiponectin*, which is correlated with insulin sensitivity (20,24), was enhanced. On the other hand, the expression of genes related to insulin resistance, such as tumor necrosis factor (*TNFα*) and heparin-binding epidermal growth factor (*HB-EGF*)-like growth factor (1,2,25), was decreased in $PLC\delta1^{-/-}$ mice.

In BAT of $PLC\delta1^{-/-}$ mice at both ages 8 and 24 weeks, the expression of thermogenic genes *UCP1* and PPARγ coactivator 1α (*PGC1α*) (5,6) was increased (Fig. 4*B*). The expression of fatty acid synthase (*Fasn*) and adrenergic receptor β3 (*Adrb3*) was also enhanced in BAT of $PLC\delta1^{-/-}$ mice (Supplementary Fig. 2*B*). These data, along with the gross appearance of BAT (Fig. 1*D*), suggest that the

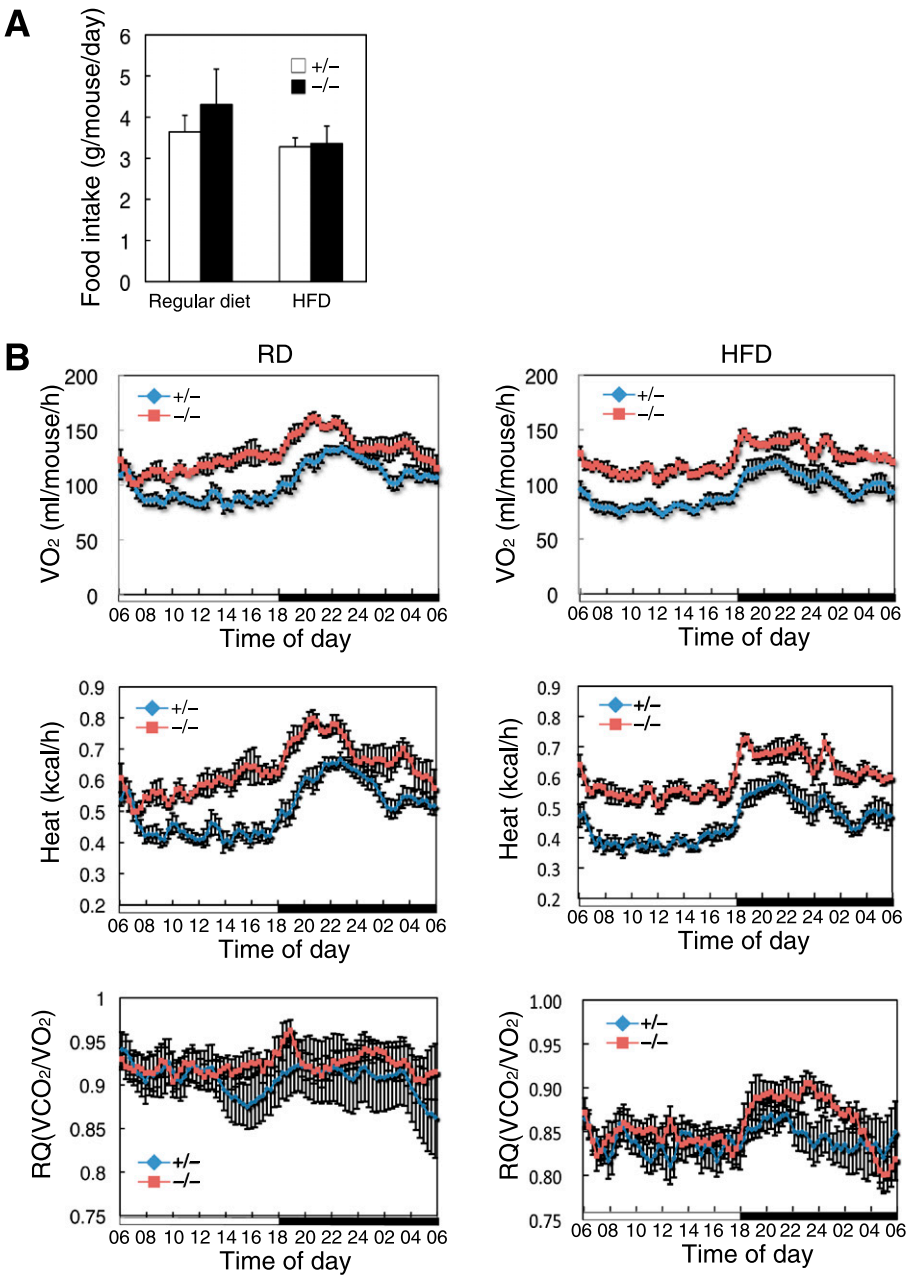

FIG. 3. Enhanced metabolic rate in *PLCδ1*$^{-/-}$ mice. *A*: Food intake was measured in 10-week-old *PLCδ1*$^{+/-}$ mice or *PLCδ1*$^{-/-}$ mice fed RD (n = 5) or HFD (n = 5). *B*: Oxygen consumption (VO_2) and carbon dioxide production (VCO_2) was measured by using an indirect calorimeter system in *PLCδ1*$^{+/-}$ mice fed RD (n = 8) or HFD (n = 7) or *PLCδ1*$^{-/-}$ mice fed RD (n = 8) or HFD (n = 6). We show VO_2 values as mL/mouse/h, since there is no consensus on how energy expenditure is normalized (41). Respiratory quotient (RQ) and heat production were calculated from VO_2 and VCO_2. Values are expressed as the mean ± SEM.

functions of BAT are well sustained in *PLCδ1*$^{-/-}$ mice, even after long-term HFD feeding.

In the liver of *PLCδ1*$^{-/-}$ mice, decreases in expression of genes related to glucose and lipid metabolism, such as acyl-CoA oxidase 1 (*Acox1*), carnitine palmitoyl transferase 1a (*Cpt1a*), *glucokinase*, and acyl-CoA dehydrogenase medium chain (*Acadm*), were observed at the age of 24 weeks (Fig. 4*C* and Supplementary Fig. 2*C*). Although these results are consistent with the observation that *PLCδ1*$^{-/-}$ mice are resistant to liver adiposity (Fig. 1*E*), it may be an adipose tissue–dependent secondary effect, because PLCδ1 is not expressed in the liver (Supplementary Fig. 1). Little change in gene expression was observed in muscles of *PLCδ1*$^{-/-}$ mice (Fig. 4*D*).

Hairlessness of *PLCδ1*$^{-/-}$ mice affects enhanced metabolic rate. We have reported that *PLCδ1*$^{-/-}$ mice have a hair defect (16). Because there are limited data on the effect of hairlessness on metabolic rate, we studied this relationship using nude mice and C57BL/6 mice with hair removed. As shown in Supplementary Fig. 3, nude mice and mice with hair removed showed increases in oxygen consumption and heat production compared with control mice, indicating that hairlessness at least partially affects metabolic rate through the change in thermogenesis.

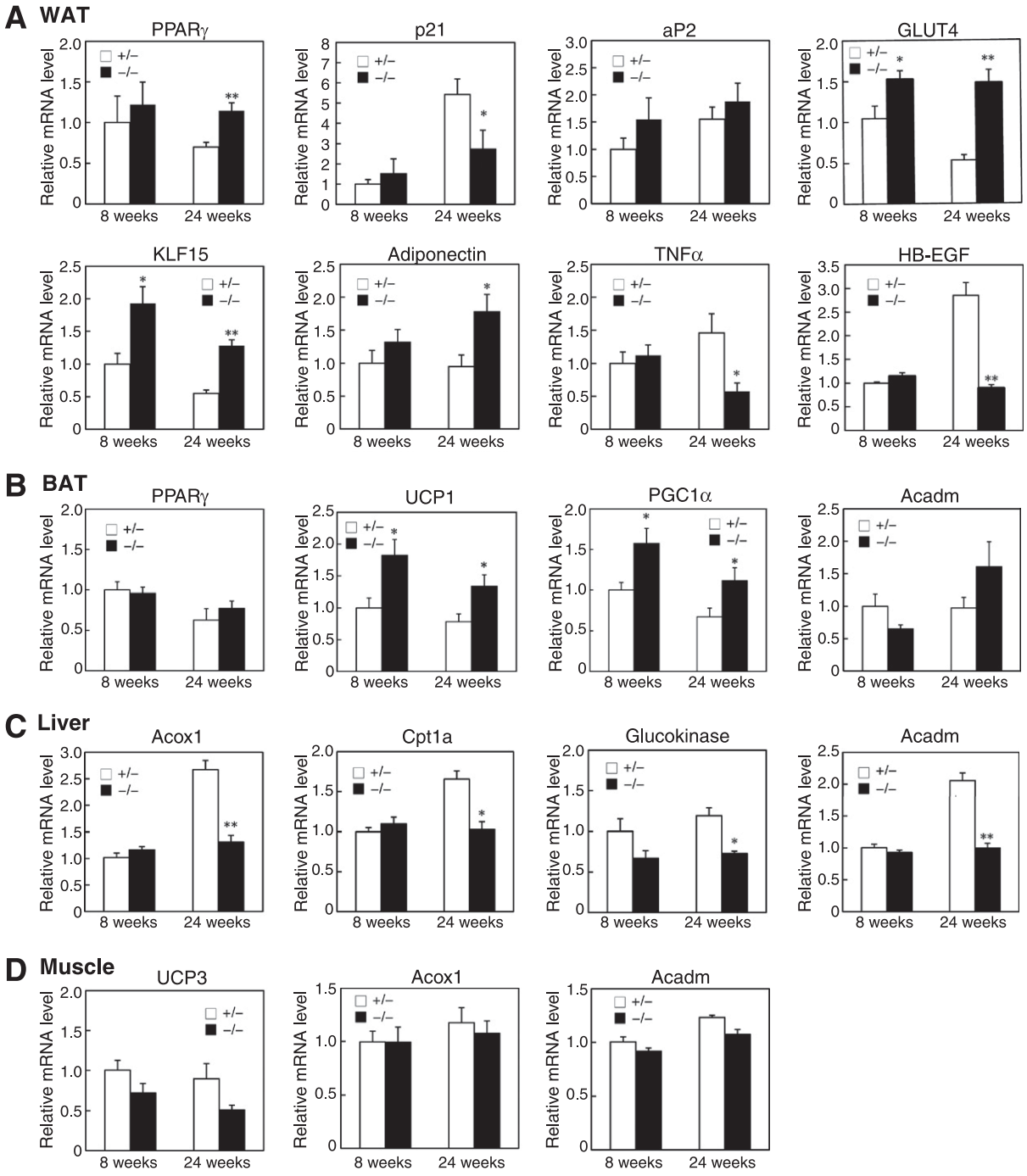

FIG. 4. Gene expression patterns of *PLCδ1*$^{-/-}$ adipose tissues show improved glucose and lipid metabolism on HFD. *A*: *PPARγ2*, *p21*, *aP2*, *GLUT4*, *KLF15*, *adiponectin*, *TNFα*, and *HB-EGF* mRNA levels in eWAT of 8-week-old *PLCδ1*$^{+/-}$ mice (n = 7) or *PLCδ1*$^{-/-}$ mice (n = 11), or 24-week-old *PLCδ1*$^{+/-}$ mice (n = 9) or *PLCδ1*$^{-/-}$ mice (n = 8) were detected by qRT-PCR. *B*: *PPARγ2*, *UCP1*, *PGC1α*, and *Acadm* mRNA levels in BAT of 8-week-old *PLCδ1*$^{+/-}$ mice (n = 9) or *PLCδ1*$^{-/-}$ mice (n = 11), or 24-week-old *PLCδ1*$^{+/-}$ mice (n = 9) or *PLCδ1*$^{-/-}$ mice (n = 8) were detected. *C*: *Acox1*, *Cpt1a*, *glucokinase*, and *Acadm* mRNA levels in the liver of 8-week-old *PLCδ1*$^{+/-}$ mice (n = 10) or *PLCδ1*$^{-/-}$ mice (n = 6), or 24-week-old *PLCδ1*$^{+/-}$ mice (n = 6) or *PLCδ1*$^{-/-}$ mice (n = 5) were detected. *D*: *UCP3*, *Acox1*, and *Acadm* mRNA levels in gastrocnemial muscles of 8-week-old *PLCδ1*$^{+/-}$ mice (n = 10) or *PLCδ1*$^{-/-}$ mice (n = 6), or 24-week-old *PLCδ1*$^{+/-}$ mice (n = 6) or *PLCδ1*$^{-/-}$ mice (n = 5) were detected. Values are normalized to *36B4* as an internal control. The quantity in 8-week-old *PLCδ1*$^{+/-}$ mice is defined as 1.0, and relative values are expressed as the mean ± SEM. *$P < 0.05$, **$P < 0.005$.

PLCδ1 negatively regulates adaptive thermogenesis. A more important question is whether PLCδ1 is directly involved in thermogenesis. We first compared the UCP1 expression in BAT mitochondria from 27-week-old mice fed HFD. The protein levels of UCP1 as well as Tim23, an inner mitochondrial membrane protein, and heat shock protein (HSP)-60 were extremely enhanced in BAT of *PLCδ1*$^{-/-}$ mice (Fig. 5*A*). Amount of mitochondrial DNA was also increased in *PLCδ1*$^{-/-}$ mice (Supplementary Fig. 3). We next examined the change in expression of *PLCδ1* mRNA in BAT from *PLCδ1*$^{+/-}$ mice placed in cold surroundings (4°C) for 3 h. As predicted, the expression levels

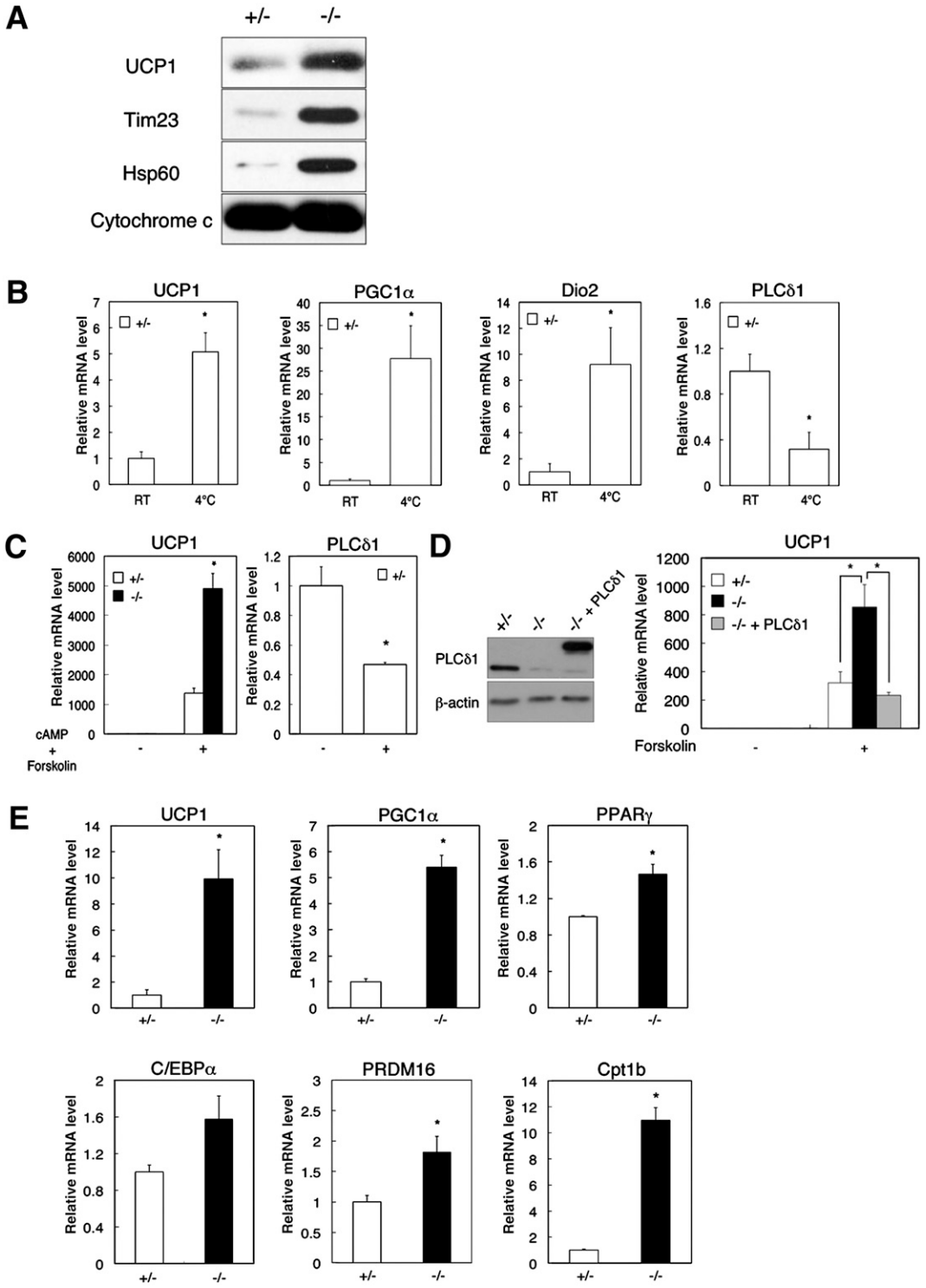

FIG. 5. PLCδ1 is involved in adaptive thermogenesis. *A*: Expressions of UCP1, Tim23, and HSP60 in BAT mitochondria of 8-week-old *PLCδ1*$^{+/-}$ mice (n = 3) or *PLCδ1*$^{-/-}$ mice (n = 3) fed with HFD were examined by Western blot analysis. BAT mitochondria were isolated by a Mitochondria Isolation Kit for Tissue (Thermo Scientific, Waltham, MA). Cytochrome c was used as the loading control. *B*: *PLCδ1* mRNA expression is decreased in BAT of cold-exposed mice. Expression levels of *UCP1*, *DIO2*, *PGC1α*, and *PLCδ1* in BAT before (RT) or after cold exposure (4°C) of 10-week-old *PLCδ1*$^{+/-}$ mice fed RD (n = 3) for 3 h were analyzed by qRT-PCR. *C*: Expression levels of *UCP1* and *PLCδ1* in immortalized brown adipocytes after induction of thermogenesis were analyzed by qRT-PCR. Differentiated *PLCδ1*$^{+/-}$ or *PLCδ1*$^{-/-}$ immortalized brown adipocytes were treated with (+) or without (−) cAMP and forskolin for 4 h. *D*: Ectopic expression of *PLCδ1* downregulated the expression of *UCP1* induced by thermogenesis. *PLCδ1*$^{-/-}$ immortalized brown adipocytes were infected with PLCδ1 retrovirus ($^{-/-}$+PLCδ1) or vector retrovirus ($^{+/-}$ or $^{-/-}$), and the *UCP1* expression levels induced by thermogenesis with forkolin were examined. Expression of PLCδ1 was confirmed by Western blotting. β-Actin was used as the loading control. *E*: Expression levels of *UCP1*, *PGC1α*, *PPARγ*, *C/EBPα*, *PRDM16*, and *CPT1b* in immortalized brown preadipocytes after differentiation were measured by qRT-PCR. Values are normalized to *36B4* as an internal control. The quantity in BAT before cold exposure of 10-week-old *PLCδ1*$^{+/-}$ mice (*B*) or differentiated *PLCδ1*$^{+/-}$ immortalized brown adipocytes (*C* and *E*) is defined as 1.0, and relative values are expressed as the mean ± SEM. *$P < 0.05$.

of thermogenic genes *UCP1*, deiodinase iodothyronine type II (*DIO2*), and *PGC1α* in BAT were increased by cold exposure (5,6,26,27) (Fig. 5*B*). In contrast, interestingly, the expression level of *PLCδ1* in BAT of *PLCδ1*$^{+/-}$ mice was decreased by cold exposure (Fig. 5*B*), strongly suggesting that PLCδ1 has a role in cold exposure–induced thermogenesis.

Similar results were obtained by using immortalized brown preadipocytes. Immortalized brown preadipocytes from *PLCδ1*$^{+/-}$ and *PLCδ1*$^{-/-}$ mice littermates were developed, differentiated, and then treated with cAMP and forskolin to induce thermogenesis (27). It is worth noting that the increase in *UCP1* expression is more remarkable in *PLCδ1*$^{-/-}$ immortalized brown adipocytes than in *PLCδ1*$^{+/-}$ adipocytes (Fig. 5*C*) and that this phenomenon is independent from hairlessness. With an inverse correlation, the expression of *PLCδ1* was reduced by induction of thermogenesis. Furthermore, the enhancement of *UCP1* expression in *PLCδ1*$^{-/-}$ adipocytes induced by thermogenesis was canceled by ectopic expression of *PLCδ1* in *PLCδ1*$^{-/-}$ immortalized brown adipocytes (Fig. 5*D*). These results clearly indicate that PLCδ1 is especially involved in adaptive thermogenesis in BAT and immortalized brown adipocytes and thereby in energy expenditure.

PLCδ1 inhibits differentiation of immortalized brown preadipocytes. We next tried to examine the involvement of PLCδ1 in brown adipocyte differentiation in vitro. The expression of *UCP1* and *PGC1α* after differentiation was remarkably enhanced in *PLCδ1*$^{-/-}$ adipocytes (Fig. 5*E*). The expression of *PPARγ*, PR domain containing 16 (*PRDM16*), and *Cpt1b* was also increased in *PLCδ1*$^{-/-}$ adipocytes. These data suggest that PLCδ1 is negatively involved in the regulation of *UCP1* or *PGC1α* expression in differentiation.

PLCδ1 positively regulates differentiation of 3T3L1 preadipocyte and WAT SVF cells. We next examined the effect of PLCδ1 on differentiation of WAT in vitro. Two sequence segments of PLCδ1 for RNA interference effectively reduced PLCδ1 expression in 3T3L1 preadipocytes by infection of the retrovirus (Fig. 6*A*). In *PLCδ1-KD* 3T3L1 adipocytes, the accumulation of lipid droplets was largely inhibited compared with cells infected by control retrovirus (Fig. 6*B*). In contrast, when PLCδ1 was ectopically expressed into 3T3L1 preadipocytes by the retrovirus (Fig. 6*C*), lipid accumulation after the induction of adipocyte differentiation was promoted (Fig. 6*D*), indicating that PLCδ1 positively regulates the differentiation of 3T3L1 preadipocytes.

We next examined the gene expression patterns during differentiation of *PLCδ1KD* 3T3L1 preadipocytes (Fig. 6*E*). Although expression levels of early differentiation genes, such as *C/EBPδ* and *C/EBPβ*, seemed to be similar between control and *PLCδ1KD* 3T3L1 preadipocytes, the expression levels of *PPARγ* and *C/EBPα* were markedly decreased in *PLCδ1KD* 3T3L1 preadipocytes at days 3 and 6 after differential induction. Similarly, remarkable decreases in expression of *KLF15*, *GLUT4*, *aP2*, and *resistin* were detected. These data suggest that PLCδ1 has important roles in the differentiation of 3T3L1 preadipocytes around from the early stage to the middle stage.

We further examined the effect of PLCδ1 on adipogenesis using WAT SVF from mice. SVF is considered to be an enriched fraction of stem cells in WAT (21). SVF was first isolated and then differentiated into adipocytes. Interestingly, lipid accumulation in *PLCδ1*$^{-/-}$ WAT SVF was reduced to less than half of that in *PLCδ1*$^{+/-}$ SVF (Fig. 6*F*). FACS analysis indicated that the cell number of WAT SVF and population of lineage-negative (Ter119$^-$, CD45$^-$) cells in WAT SVF were almost the same between *PLCδ1*$^{-/-}$ and *PLCδ1*$^{+/-}$ WAT SVF, indicating that the reduced lipid accumulation of *PLCδ1*$^{-/-}$ WAT SVF was caused by the differentiation potential, but not the number of lineage-negative cells. Taken together, these results indicate that PLCδ1 positively regulates both adipogenesis and hypertrophic lipid accumulation in WAT model culture cells.

Impaired WAT development at the early postnatal stage of *PLCδ1*$^{-/-}$ mice. We further tried to examine the role of PLCδ1 in WAT development in mice. To exclude the effect of hairlessness of *PLCδ1*$^{-/-}$ mice, we analyzed mice at 6 days of age, before hair growth. Even as early as 6 days of age, inguinal WAT mass was significantly decreased in *PLCδ1*$^{-/-}$ mice (Fig. 7*A*). We also detected the decreases in the expression of *C/EBPβ*, *PPARγ*, *C/EBPα*, *KLF15*, *aP2*, *GLUT4*, and lipoprotein lipase (*LPL*) in inguinal WAT of *PLCδ1*$^{-/-}$ mice compared with those of *PLCδ1*$^{+/-}$ mice. These expression profiles are generally consistent with those of 3T3L1 cells, indicating that PLCδ1 is involved in adipose development and has functional roles in adipose tissues in mice.

PKCβI, PKCε, and NFATc4 are downstream targets of PKCδ1 in adipocyte differentiation. To provide mechanisms downstream of PLCδ1 in differentiation of adipocytes, we focused on PKC and NFAT, which are targets of the second messengers diacylglycerol and/or inositol 1,4,5-triphosphate/calcium. Among PKC isozymes, PKCβ—a conventional type of PKC—was reported to be involved in adipocyte differentiation (28), and PKCβKO mice were leaner and more resistant to HFD-induced obesity (29). When PKCβ is activated, PKCβ is translocated from the cytosol to the plasma membrane (28). An increase in PKCβI expression at the plasma membrane was significantly observed at 48 h after the induction in control 3T3L1 adipocytes, whereas this increase was less detected in PLCδ1KD adipocytes (Fig. 8*A*). In addition, PKCε—a novel type of PKC—began to be expressed in the nuclei and is required for adipocyte differentiation (30,31), and functional ablation of PKCε in mice show improved glucose homeostasis in models of type 2 diabetes (32). PKCε expression was increased in the nuclei of control 3T3L1 cells, but not in PLCδ1KD cells at 48 h after the induction (Fig. 8*B*).

Mice with the NFATc2/NFATc4 gene disruption exhibit defects in fat accumulation and are protected from diet-induced obesity (33). Immunostaining indicated that NFATc4 expressions were induced in control 3T3L1 adipocytes, whereas they were less induced in PLCδ1KD adipocytes (Fig. 8*C*). Taken together, we identified for the first time PKCβI, PKCε, and NFATc4 as downstream molecules of PLCδ1 in adipogenesis of 3T3L1 cells.

DISCUSSION

Phosphoinositol (PI) 3-kinase–mediated phosphorylation of insulin receptor substrate or Akt is essential for GLUT4 translocation and glucose uptake (34–36). Therefore, we predicted that PLCδ1 is directly involved in insulin signaling. However, we have not found any relation between PLCδ1 and PI 3-kinase, such as increased phosphorylation of Akt in WAT of *PLCδ1*$^{-/-}$ mice. Therefore, the enhanced insulin sensitivity observed in *PLCδ1*$^{-/-}$ mice may be explained by the condition of less obesity.

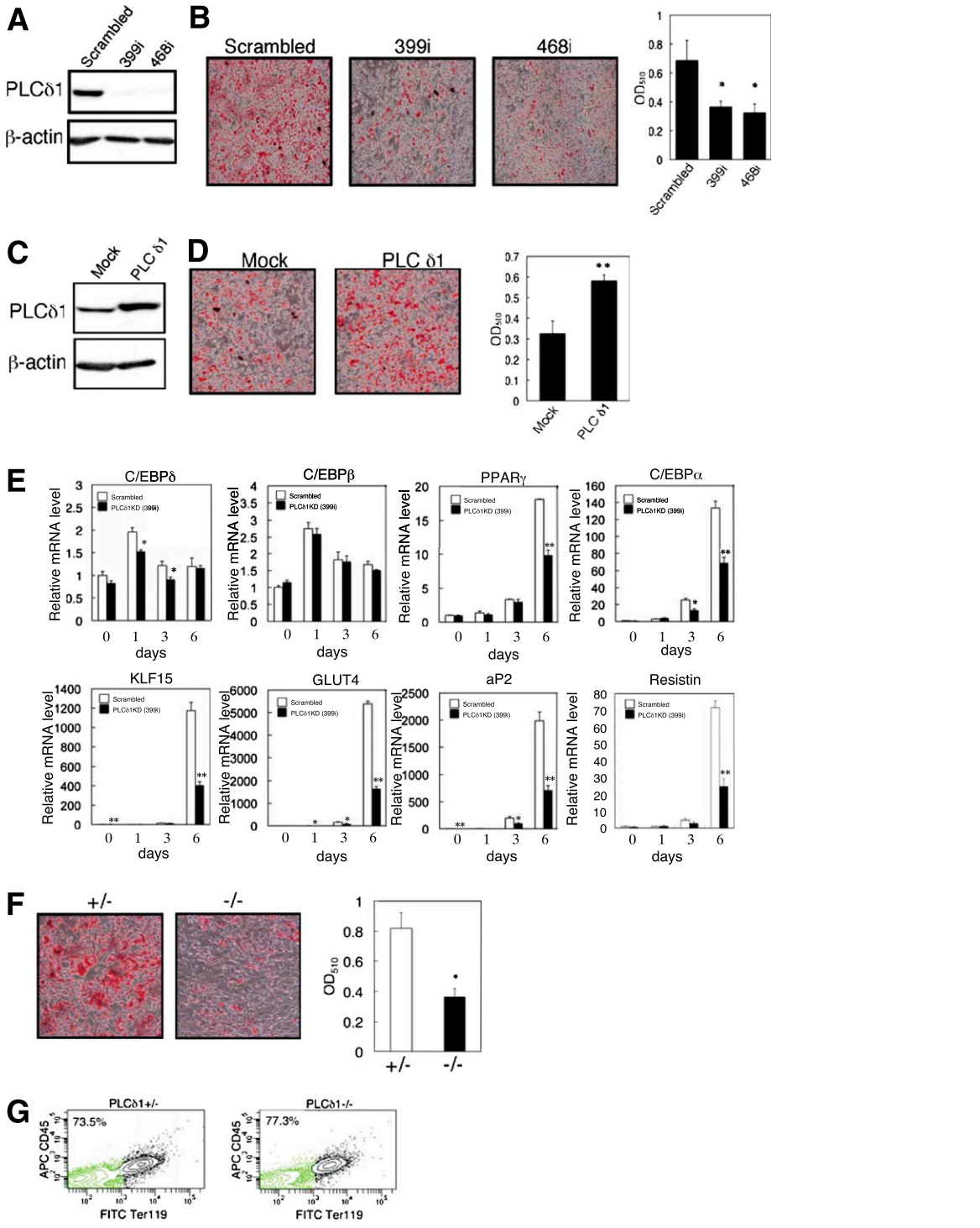

FIG. 6. PLCδ1 directly regulates adipocyte differentiation. *A* and *B*: *PLCδ1KD* in 3T3L1 cells inhibits adipogenesis. 3T3L1 cells were infected with PLCδ1 RNAi retrovirus (399i or 468i) or control retrovirus (Scrambled), and the expression levels of PLCδ1 were determined by Western blotting (*A*). β-Actin was used as loading control. Differentiated adipocytes were stained with Oil Red O. Oil Red O extracted with isopropanol was measured at OD_{510}. *C* and *D*: Ectopic expression of PLCδ1 promotes adipogenesis. 3T3L1 cells were infected with PLCδ1 retrovirus (PLCδ1) or vector retrovirus (Mock), and the PLCδ1 expression levels were confirmed by Western blotting (*C*). Adipocyte differentiation was induced, and lipid droplets were stained with Oil Red O. *E*: Expression levels of adipogenesis-related gene in scrambled and *PLCδ1KD* (399i) 3T3L1 cells during the differentiation (days 0, 1, 3, and 6) were measured by qRT-PCR. Values are normalized to *36B4* as an internal control. The quantity of scrambled cells (differentiation day 0) is defined as 1.0. *F*: $PLC\delta1^{-/-}$ WAT SVF showed impaired lipid accumulation. SVF was isolated and then differentiated. Lipid accumulation was verified by Oil Red O staining and quantified by extraction with isopropanol. *G*: Lineage negative ($Ter119^-$/$CD45^-$, green areas) population in $PLC\delta1^{-/-}$ WAT SVF was compared with that in $PLC\delta1^{+/-}$ WAT SVF by FACS analysis (the former is 77.2 ± 0.4% and the latter is 73.0 ± 3.2%). Relative values are expressed as the mean ± SEM. *$P < 0.05$, **$P < 0.005$. (A high-quality digital representation of this figure is available in the online issue.)

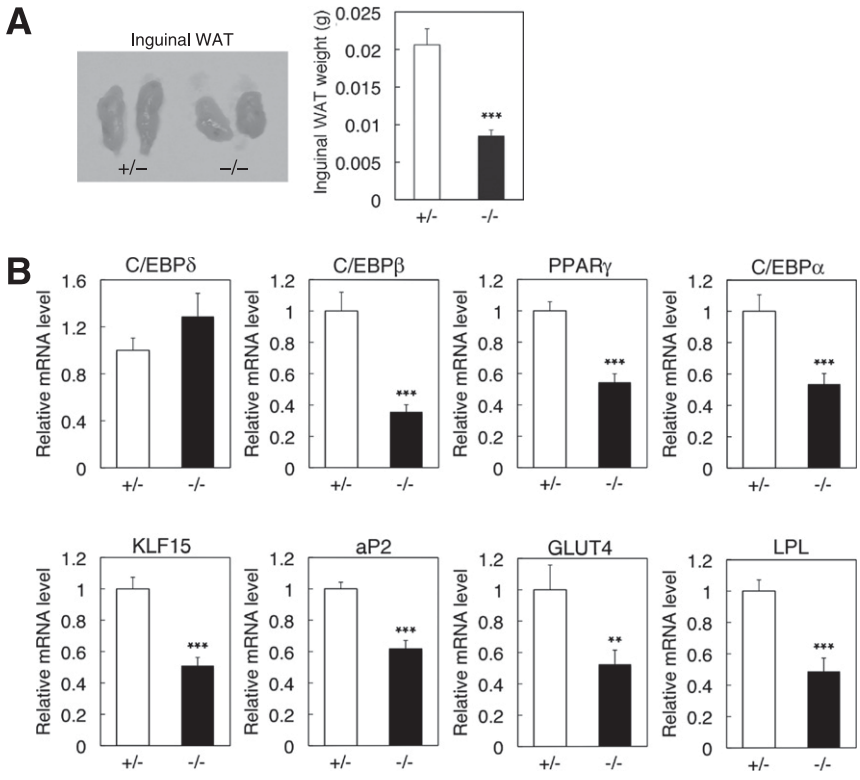

FIG. 7. Impaired WAT development at an early postnatal stage of *PLCδ1*$^{-/-}$ mice. *A*: Weight of inguinal WAT from 6-day-old *PLCδ1*$^{+/-}$ mice (n = 12) or *PLCδ1*$^{-/-}$ mice (n = 16). *B*: mRNA levels of *C/EBPδ*, *C/EBPβ*, *PPARγ*, *C/EBPα*, *KLF15*, *aP2*, *GLUT4*, and *LPL* in inguinal WAT from 6-day-old *PLCδ1*$^{+/-}$ mice (n = 7) or *PLCδ1*$^{-/-}$ mice (n = 9) were measured by qRT-PCR. Values are normalized by *36B4* as an internal control. The quantity in 6-day-old *PLCδ1*$^{+/-}$ mice is defined as 1.0, and relative values are expressed as the mean ± SEM. **$P < 0.005$, ***$P < 0.0005$.

When mice are exposed to cold temperatures, upregulation of *UCP1* and *DIO2* in BAT is essential for adaptive thermogenesis to maintain body temperature; cold-exposed *DIO2*$^{-/-}$ mice became hypothermic because of impaired BAT thermogenesis (26). *UCP1*$^{-/-}$ mice are also cold sensitive and show temperature-dependent obesity (37,38). It is noteworthy that PLCδ1 expression had dramatically decreased in BAT from mice exposed to cold and immortalized brown preadipocytes treated with thermogenic inducers, and it showed an inverse correlation with the upregulation of thermogenic genes such as *UCP1* and *PGC1α* (Fig. 5*B–D*). These observations indicate that PLCδ1 participated in adaptive thermogenesis mediated by *UCP1* and *PGC1α* in a physiological manner.

In vitro analysis further confirmed that PLCδ1 regulates adipogenesis. We indicated that PLCδ1 negatively regulates *UCP1* or *PGC1α* expression during differentiation of brown adipocytes (Fig. 5*E*), whereas PLCδ1 positively regulates differentiation of preadipocytes in WAT culture cells (Fig. 6*B*, *E*, and *F*). The opposing regulation of PLCδ1 in the WAT and BAT models seems interesting. Detailed future works could provide insights into the mechanism of differentiation decision or conversion between WAT and BAT.

A similar gene expression pattern with 3T3L1 cells was observed in inguinal WAT of 6-day-old *PLCδ1*$^{-/-}$ mice, at which age the effect of hair is negligible. This result shows that PLCδ1 is involved in adipose development in adipose tissues in mouse pups. On the other hand, the elevation of *PPARγ*, *GLUT4*, or *KLF15*, and reduced expression of genes related to WAT hypertrophy or insulin resistance in the case of 24-week-old *PLCδ1*$^{-/-}$ mice fed with HFD (Fig. 4*A*), indicate that *PLCδ1*$^{-/-}$ WAT sustains normal adipose functions, even under diet-induced hypertrophic conditions. A similar observation was reported in IκB kinase ε (*IKKε*)$^{-/-}$ mice. IKK positively regulates the nuclear factor (NF)-κB pathway by phosphorylation and release of inhibitory IκB from NFκB. *IKKε*$^{-/-}$ mice are protected from diet-induced obesity and show increased expression of *PPARγ*, *GLUT4*, or *adiponectin* in WAT, as well as enhanced energy expenditure at the age of 22–26 weeks (39). Because NFκB is a downstream effector of PLC, a relationship between PLCδ1 and NFκB would be predicted. It is noteworthy to identify NFATc4, as well as PKCβI and PKCε, as downstream molecules of PLCδ1. PLCδ1 was recently reported to act as an anti-oncogene and regulate the expression of p21 in esophageal squamous cell carcinoma (40). Taken together with these reports, our results indicate the possibility that the loss of PLCδ1 in WAT induces a decrease in *p21* expression and inhibits the development of hypertrophy. Reduced hypertrophy development in turn results in a decrease in expression of insulin resistance–inducing genes, *TNFα*, or *HB-EGF* and increases in expression of the insulin-sensitive gene *adiponectin*.

Here, we show for the first time that PLCδ1 contributes to thermogenesis and adipogenesis, and thereby in developing obesity. It is important to further elucidate how PLCδ1 participates in these various pathways, since obesity is an important issue in present society.

ACKNOWLEDGMENTS

This work was supported by a Grant-in-Aid for General Scientific Research and a High-Tech Research Center

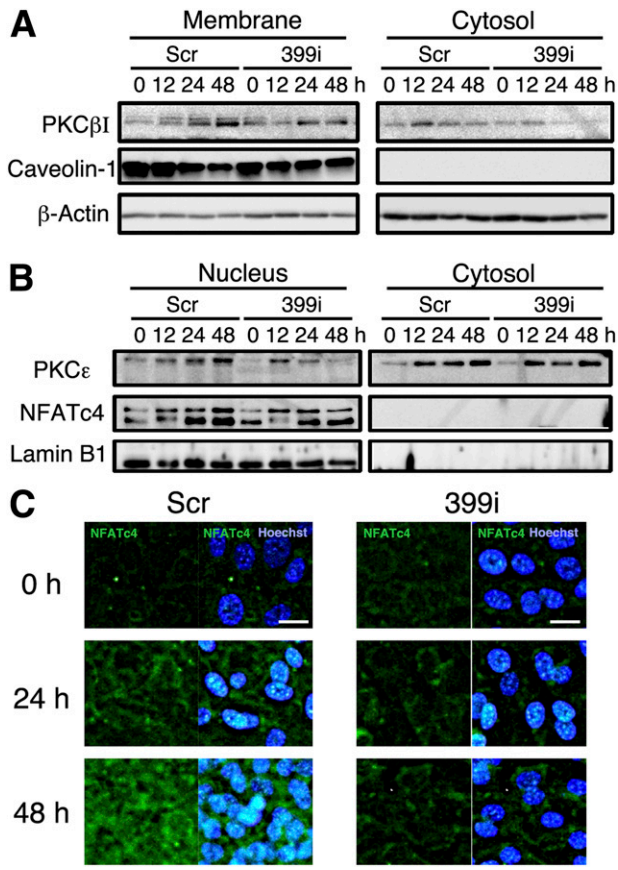

FIG. 8. KD of PKCδ1 suppressed the activation of PKCβI, PKCε, and NFATc4 during adipocyte differentiation. 3T3L1 cells infected with PLCδ1 RNAi retrovirus (399i) or control retrovirus (Scr) were induced differentiation for the indicated hours (*A–C*). *A*: Expressions of PKCβI at the plasma membrane during adipocyte differentiation were examined. The membrane and cytosolic fractions were isolated as described previously (28). Western blotting was performed with anti-PKCβI, anti–Caveolin-1, and anti–β-actin antibodies. Caveolin-1 and β-actin were used for plasma membrane marker and loading control, respectively. *B*: Nuclear expressions of PKCε during adipocyte differentiation. The nuclear and cytosolic fractions were isolated with an NE-PER Nuclear and Cytoplasmic Extraction kit according to the manufacturer's instructions. Western blotting was performed with anti-PKCε, anti-NFATc4, and antilamin B1 antibodies. Lamin B1 was used for a nuclear marker. *C*: Expressions of NFATc4 during adipocyte differentiation were examined by immunocytochemistry (42). Cells were stained with anti-NFATc4 antibody. Nuclei were stained with Hoechst 33258 (Invitrogen). Immunofluorescence microscopy images of cells with NFATc4 staining (*left*) and merged images (*right*) were obtained by fluorescence microscope Biozero (Keyence). Bars: 20 μm. (A high-quality digital representation of this figure is available in the online issue.)

Project for private universities matching the fund subsidy (to K.F.) from the Japan Ministry of Education, Culture, Sports, Science and Technology. This work was also supported in part by the Mochida Memorial Foundation for Medical and Pharmaceutical Research and Takeda Science Foundation (to K.F.). This work was carried out by the joint research program of the Institute for Molecular and Cellular Regulation, Gunma University (#22002). No other potential conflicts of interest relevant to this article were reported.

M.H. and M.S. researched data, contributed to discussion, and reviewed and edited the manuscript. R.I., R.S., T.U., and To.K. researched data and contributed to discussion. T.S. and Ta.K. researched data, contributed to discussion, and reviewed and edited the manuscript. H.Y. contributed to discussion. Y.N. contributed to discussion and reviewed and edited the manuscript. K.F. contributed to discussion, wrote the manuscript, and reviewed and edited the manuscript.

The authors thank Dr. Toshio Kitamura (Tokyo University) for providing the Plat-A cells and pMX vectors; Shoichi Matsuoka, Fumiko Yoshino, and Kaori Kanemaru (Tokyo University of Pharmacy and Life Sciences) for technical assistance; and Dr. Masataka Asagiri (University of California, San Diego) for valuable advice.

REFERENCES

1. Rosen ED, Spiegelman BM. Adipocytes as regulators of energy balance and glucose homeostasis. Nature 2006;444:847–853
2. Karastergiou K, Mohamed-Ali V. The autocrine and paracrine roles of adipokines. Mol Cell Endocrinol 2010;318:69–78
3. White UA, Stephens JM. Transcriptional factors that promote formation of white adipose tissue. Mol Cell Endocrinol 2010;318:10–14
4. Lefterova MI, Lazar MA. New developments in adipogenesis. Trends Endocrinol Metab 2009;20:107–114
5. Kozak LP, Anunciado-Koza R. UCP1: its involvement and utility in obesity. Int J Obes (Lond) 2008;32(Suppl. 7):S32–S38
6. Kajimura S, Seale P, Spiegelman BM. Transcriptional control of brown fat development. Cell Metab 2010;11:257–262
7. Tseng YH, Kokkotou E, Schulz TJ, et al. New role of bone morphogenetic protein 7 in brown adipogenesis and energy expenditure. Nature 2008;454:1000–1004
8. Farmer SR. Molecular determinants of brown adipocyte formation and function. Genes Dev 2008;22:1269–1275
9. Park KW, Halperin DS, Tontonoz P. Before they were fat: adipocyte progenitors. Cell Metab 2008;8:454–457
10. Enerbäck S. Human brown adipose tissue. Cell Metab 2010;11:248–252
11. Frontini A, Cinti S. Distribution and development of brown adipocytes in the murine and human adipose organ. Cell Metab 2010;11:253–256
12. Di Paolo G, De Camilli P. Phosphoinositides in cell regulation and membrane dynamics. Nature 2006;443:651–657
13. Martin TF. PI(4,5)$P_{(2)}$ regulation of surface membrane traffic. Curr Opin Cell Biol 2001;13:493–499
14. Suh PG, Park JI, Manzoli L, et al. Multiple roles of phosphoinositide-specific phospholipase C isozymes. BMB Rep 2008;41:415–434
15. Fukami K, Inanobe S, Kanemaru K, Nakamura Y. Phospholipase C is a key enzyme regulating intracellular calcium and modulating balance of phosphoinositides. Prog Lipid Res 2010;49:366–377
16. Nakamura Y, Fukami K, Yu H, et al. Phospholipase Cdelta1 is required for skin stem cell lineage commitment. EMBO J 2003;22:2981–2991
17. Ichinohe M, Nakamura Y, Sai K, Nakahara M, Yamaguchi H, Fukami K. Lack of phospholipase C-δ1 induces skin inflammation. Biochem Biophys Res Commun 2007;356:912–918
18. Nakamura Y, Ichinohe M, Hirata M, et al. Phospholipase C-delta1 is an essential molecule downstream of Foxn1, the gene responsible for the nude mutation, in normal hair development. FASEB J 2008;22:841–849
19. Kitamura T, Koshino Y, Shibata F, et al. Retrovirus-mediated gene transfer and expression cloning: powerful tools in functional genomics. Exp Hematol 2003;31:1007–1014
20. Mori T, Sakaue H, Iguchi H, et al. Role of Krüppel-like factor 15 (KLF15) in transcriptional regulation of adipogenesis. J Biol Chem 2005;280:12867–12875
21. Rodeheffer MS, Birsoy K, Friedman JM. Identification of white adipocyte progenitor cells in vivo. Cell 2008;135:240–249
22. Klein J, Fasshauer M, Ito M, Lowell BB, Benito M, Kahn CR. Beta(3)-adrenergic stimulation differentially inhibits insulin signaling and decreases insulin-induced glucose uptake in brown adipocytes. J Biol Chem 1999;274:34795–34802
23. Inoue N, Yahagi N, Yamamoto T, et al. Cyclin-dependent kinase inhibitor, p21WAF1/CIP1, is involved in adipocyte differentiation and hypertrophy, linking to obesity, and insulin resistance. J Biol Chem 2008;283:21220–21229
24. Kadowaki T, Yamauchi T, Kubota N, Hara K, Ueki K, Tobe K. Adiponectin and adiponectin receptors in insulin resistance, diabetes, and the metabolic syndrome. J Clin Invest 2006;116:1784–1792
25. Gustafson B, Gogg S, Hedjazifar S, Jenndahl L, Hammarstedt A, Smith U. Inflammation and impaired adipogenesis in hypertrophic obesity in man. Am J Physiol Endocrinol Metab 2009;297:E999–E1003
26. de Jesus LA, Carvalho SD, Ribeiro MO, et al. The type 2 iodothyronine deiodinase is essential for adaptive thermogenesis in brown adipose tissue. J Clin Invest 2001;108:1379–1385

27. Puigserver P, Wu Z, Park CW, Graves R, Wright M, Spiegelman BM. A cold-inducible coactivator of nuclear receptors linked to adaptive thermogenesis. Cell 1998;92:829–839
28. Zhou Y, Wang D, Li F, Shi J, Song J. Different roles of protein kinase C-betaI and -delta in the regulation of adipocyte differentiation. Int J Biochem Cell Biol 2006;38:2151–2163
29. Huang W, Bansode R, Mehta M, Mehta KD. Loss of protein kinase Cbeta function protects mice against diet-induced obesity and development of hepatic steatosis and insulin resistance. Hepatology 2009;49:1525–1536
30. Fleming I, MacKenzie SJ, Vernon RG, Anderson NG, Houslay MD, Kilgour E. Protein kinase C isoforms play differential roles in the regulation of adipocyte differentiation. Biochem J 1998;333:719–727
31. Dasgupta S, Bhattacharya S, Maitra S, et al. Mechanism of lipid induced insulin resistance: activated PKCε is a key regulator. Biochim Biophys Acta 2011;1812:495–506
32. Schmitz-Peiffer C, Laybutt DR, Burchfield JG, et al. Inhibition of PKCepsilon improves glucose-stimulated insulin secretion and reduces insulin clearance. Cell Metab 2007;6:320–328
33. Yang TT, Suk HY, Yang X, et al. Role of transcription factor NFAT in glucose and insulin homeostasis. Mol Cell Biol 2006;26:7372–7387
34. Saltiel AR. New perspectives into the molecular pathogenesis and treatment of type 2 diabetes. Cell 2001;104:517–529
35. Bernal-Mizrachi E, Fatrai S, Johnson JD, et al. Defective insulin secretion and increased susceptibility to experimental diabetes are induced by reduced Akt activity in pancreatic islet beta cells. J Clin Invest 2004;114:928–936
36. Wang Q, Somwar R, Bilan PJ, et al. Protein kinase B/Akt participates in GLUT4 translocation by insulin in L6 myoblasts. Mol Cell Biol 1999;19:4008–4018
37. Enerbäck S, Jacobsson A, Simpson EM, et al. Mice lacking mitochondrial uncoupling protein are cold-sensitive but not obese. Nature 1997;387:90–94
38. Feldmann HM, Golozoubova V, Cannon B, Nedergaard J. UCP1 ablation induces obesity and abolishes diet-induced thermogenesis in mice exempt from thermal stress by living at thermoneutrality. Cell Metab 2009;9:203–209
39. Chiang SH, Bazuine M, Lumeng CN, et al. The protein kinase IKKepsilon regulates energy balance in obese mice. Cell 2009;138:961–975
40. Fu L, Qin YR, Xie D, et al. Characterization of a novel tumor-suppressor gene PLC delta 1 at 3p22 in esophageal squamous cell carcinoma. Cancer Res 2007;67:10720–10726
41. Kaiyala KJ, Schwartz MW. Toward a more complete (and less controversial) understanding of energy expenditure and its role in obesity pathogenesis. Diabetes 2011;60:17–23
42. Yamaguchi H, Takeo Y, Yoshida S, Kouchi Z, Nakamura Y, Fukami K. Lipid rafts and caveolin-1 are required for invadopodia formation and extracellular matrix degradation by human breast cancer cells. Cancer Res 2009;69:8594–8602